

Axisymmetric granular collapse: a transient 3D flow test of visco-plasticity

Laurent Lacaze* and Rich R. Kerswell†

Department of Mathematics, University Walk, Bristol University, Bristol BS8 1TW, U. K.

(Dated: January 14, 2009)

A viscoplastic continuum theory has recently been proposed to model dense, cohesionless granular flows (Jop *et al.* *Nature*, **441**, 727, 2006). We confront this theory for the first time with a transient, 3-dimensional flow situation - the simple collapse of a cylinder of granular matter onto a horizontal plane - by extracting stress and strain rate tensors directly from soft particle simulations. These simulations faithfully reproduce the different flow regimes and capture the observed scaling laws for the final deposit. Remarkably, the theoretical hypothesis that there is a simple stress-strain rate tensorial relationship does seem to hold over the whole flow during the evolution even close to the rough boundary provided the flow is dense enough. These encouraging results suggest viscoplastic theory is more generally applicable to transient, multi-directional, dense flows and open the way for quantitative predictions in real applications.

A predictive theory for the flow of granular media remains a major objective for the physics community with industrial facilities handling granular materials operating well below design efficiency and destructive natural phenomena such as snow avalanches, landslides and debris flows difficult to safeguard against [1, 18]. A central difficulty is the behaviour of granular materials is not easily classified as being either solid, liquid or gas-like with multiple phases sometimes appearing simultaneously. In particular, the solid-liquid regime where there is a dense granular flow coexisting with a stopped solid-like deposit remains a considerable modelling challenge. In industrial (e.g. silo flow) and geophysical (e.g. avalanches) applications, the size of the constituent particles ($\gg \mu\text{m}$) means that thermal effects are completely negligible compared to external forces such as gravity [1]. The dynamics are then dominated by the inelastic collisions between particles which involve highly nonlinear frictional forces. As a further complication, there is typically no scale separation between the microscopic (granular) dimension and the lengthscales over which the flow varies. Notwithstanding this, a visco-plastic continuum theory is starting to emerge [2] for dense granular media built upon the observations that a non-zero shear rate is needed to initiate movement and, once moving, there is a complicated flow dependence on the shear rate. At the heart of this theory is a dimensionless inertial number, I which is a *local* ratio of a macroscopic deformation timescale to an inertial timescale [19]. Numerical simulations of a simple sheared cell [3, 4] had identified the importance of this quantity which was subsequently realised to be also highly relevant to other flows with a single shear plane [5]. Jop *et al.* [2] then provided a multidimensional generalisation by defining $I := |\dot{\gamma}|d/\sqrt{P}/\rho$ and tensorializing the stress-strain relationship to

$$\tau_{ij} = \eta \hat{\gamma}_{ij}, \quad \text{with} \quad \eta := \mu(I)P/|\dot{\gamma}|, \quad (1)$$

where P is the isotropic pressure, $|\dot{\gamma}| := \sqrt{\frac{1}{2}\hat{\gamma}_{ij}\hat{\gamma}_{ij}}$ is the second invariant of the strain rate tensor $\hat{\gamma}_{ij} := u_{i,j} + u_{j,i}$, $u_{i,j}$ is the j th derivative of the i th velocity compo-

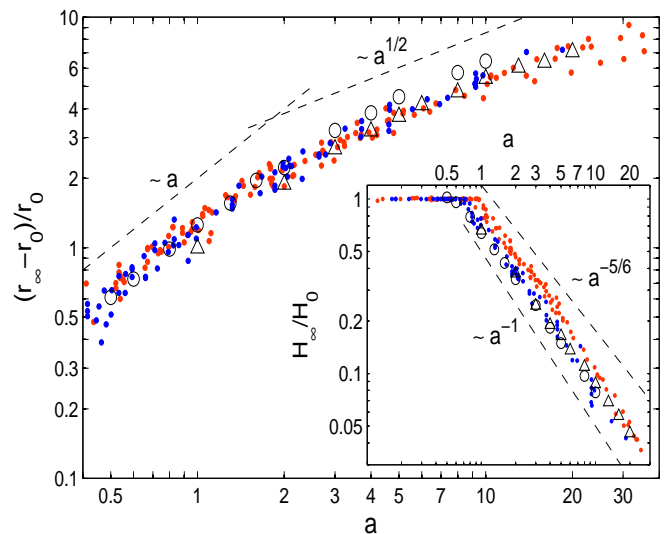


FIG. 1: Discrete element simulations and experimental data of the non-dimensional runout $(r_\infty - r_0)/r_0$ and maximum final height H_∞/H_0 as a function of a . Open symbols correspond to numerical results for $d = 2\text{mm}$, $r_0 = 2\text{cm}$ (Δ) and $r_0 = 3.5\text{cm}$ (\circ) ($\mu_m = 0.5$) and dots are experimental results: data from Lajeunesse *et al.* [6] (dark/blue) and from Lube *et al.* [7] (light/red). ([6] claims $h_\infty/h_0 \sim a^{-1}$ whereas [7] quote $\sim a^{-5/6}$.) The symbol size of the numerical data indicates the variability over repeated runs.

nent, d is the particle diameter, ρ is the particle density, $\tau_{ij} := \sigma_{ij} + P\delta_{ij}$ is the deviatoric stress tensor (σ_{ij} being the stress tensor), η is the viscosity and μ a friction coefficient. By solving the continuum equations with the rheology (1), Jop *et al.* achieved predictions within 15% of actual flow velocities for a steady, unidirectional granular flow sheared in both cross-stream directions.

In this letter, we confront this new theory with a transient 3-dimensional situation where the flow is not unidirectional to test its applicability to real flows of practical interest. The flow situation studied is the intriguingly simple table-top flow generated by a collapsing granu-

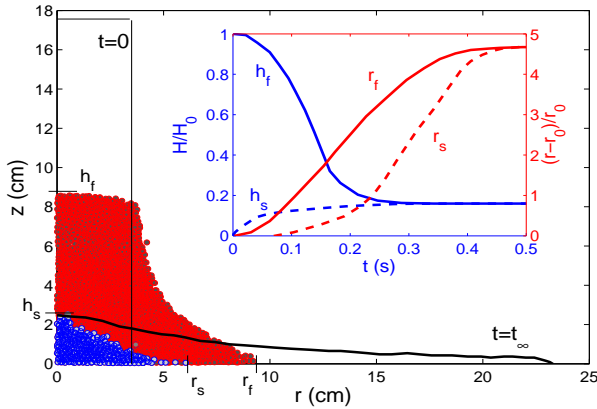


FIG. 2: Granular pile and static interface evolution as a function of time in the (r, z) plane ($a = 5$, $r_0 = 3.5\text{cm}$, $\mu_m = 0.5$) from DEM. Thick line corresponds to the final deposit and the thin line is the initial configuration. An intermediate profile is also shown at $t = 0.14\text{ s}$ to illustrate the growing stationary deposit (dark/blue; height h_s , radius r_s) and the flowing dense layer (light/red; height h_f , radius r_f). The inset shows how these two heights and radii evolve over time (normalised using the initial height H_0 and radius r_0).

lar cylindrical column [6, 7]. This is a particularly good test case because the initial condition is well-defined, the subsequent dynamics are rich, combining a number of different flow regimes, and the flow duration is short enough that realistic discrete element simulations (DEM) can be done to calculate the stress and strain rates everywhere at any given time.

The collapsing column experiment consists of releasing a stationary cylinder of granules so that they fall and spread out on a horizontal surface. If the aspect ratio $a := h_0/r_0$ (h_0 and r_0 being the height and radius of the initial cylinder) of the column is small ($\lesssim 2$), the collapse starts at the column edge and propagates inwards either stopping before the top is totally eroded away (so the final maximum height $h_\infty = h_0$) or eventually leading to a complete collapse ($h_\infty < h_0$). If $a \gtrsim 2$, the column collapses instantaneously as a whole with three flow phases evident: I, the free-fall regime where the top of the cylinder falls ballistically; II, a heap regime where moving grains flow over a growing inclined stationary deposit; and III, shallow layer regime where the motion is dominantly horizontal. Simple power laws exist for the runout, $(r_\infty - r_0)/r_0 \sim a^{1/2}$ [6, 7], and maximum height $h_\infty/h_0 \sim a^{-1}$ [6] or $\sim a^{-5/6}$ [7] of the final deposit (see Figure 1) with only the numerical prefactors appearing material-dependent [8]. The observation $h_\infty \sim h_0/a = r_0$ is particularly striking as this implies that the final height becomes *independent* of the initial height for a sufficiently tall starting column. Efforts to explain these scalings have either concentrated on shallow layer modelling [9–11] or 2-dimensional DEM (hard

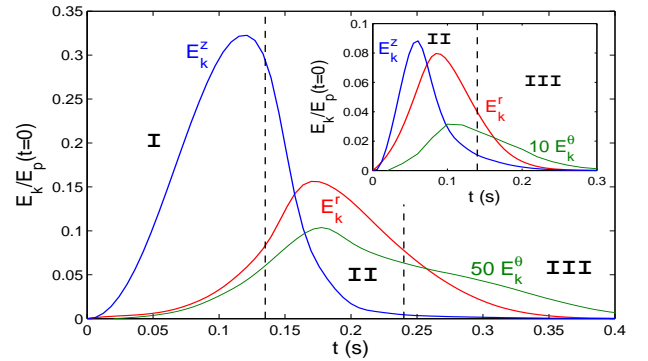


FIG. 3: Evolution of the radial kinetic energy E_k^r (red), azimuthal kinetic energy E_k^θ (green) and vertical kinetic energy E_k^z (blue) where $E_k^\alpha := \sum_{n=1}^N \frac{1}{2} m u_{\alpha,n}^2$, $u_{\alpha,n}$ is the velocity of the n th particle in the α ($= r, \theta$ or z) direction for the run of figure 2. N is the total number of particles, m is the mass of each particle and g is gravity. *Inset*: same quantities but for $a = 1$ where there is no free-fall regime I. (All quantities have been non-dimensionalised by the initial potential energy $E_p(t=0)$).

[12, 13] and soft [14] particle).

Measuring pointwise stress and strain rates for this flow in the laboratory is impractical so 3-dimensional discrete element modelling (DEM) was carried out [20]. Up to 2×10^5 monodisperse, cohesionless, frictional, inelastic spheres of $d = 2\text{mm}$ diameter randomly packed into cylinders with aspect ratio $a \in [0.5, 20]$ were released over a roughened horizontal plane on which a monolayer of the same spheres was glued. The code used a Hertz-Mindlin theory to model the contact physics of colliding (soft) spheres (see [15] for details). The results were insensitive (see [13, 15]) to coefficient of restitution e provided e is not too close to 1 so this was taken nominally as 0.5 whereas the coefficient of (microscopic) friction μ_m was varied. Calculations were mainly performed with initial radii of $r_0 = 2\text{cm}$ or 3.5cm implying a ‘granularity’ of 10 or 17.5 spheres respectively across a radius compared to $\gtrsim 50$ in experiments. Figure 1 shows that the DEM captures the same scaling laws as seen in experiments, with the $r_0 = 3.5\text{cm}$ data having a slightly larger runout prefactor than the $r_0 = 2\text{cm}$ data. This discrepancy is well within the experimental data spread but is significant compared to the variability of repeated ‘identical’ numerical experiments (the columns were filled by randomly dropping granules from a fixed height). Two tests for larger values of r_0 ($r_0 = 6\text{cm}$, $a = 1$ and $r_0 = 7.5\text{cm}$, $a = 0.5$, however, reproduced the $r_0 = 3.5\text{cm}$ runout data, indicating that, at least for small a , the effects of granularity on the collapse are lost within the numerical error bars at this r_0 . Figure 2 shows a typical collapse for $a = 5$ calculated using DEM. An intermediate flow state is characterised by its upper moving free surface and the lower static interface which delineates the grow-

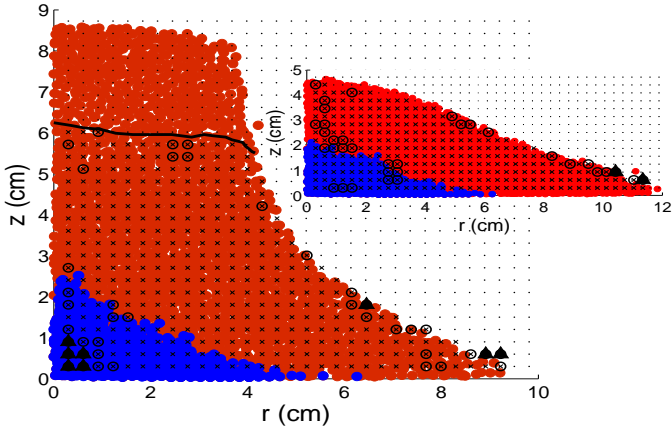


FIG. 4: The grid over which data was collected for $t = 0.14s$ and $a = 5$ (inset $t = 0.18s$). Symbol positions indicate the centres of the $3d \times 3d$ averaging boxes and the type of symbol the misalignment angle ϕ between the principal axes of $\boldsymbol{\tau}$ and $\dot{\boldsymbol{\gamma}}^c$; $\phi < 5^\circ$ crosses, $5^\circ < \phi < 10^\circ$ crosses with circles, and $\phi > 10^\circ$ solid triangles. The pressure $P < 0.05P_{max}$ above the black line and the blue ‘stopped’ region is defined by the threshold $|v| < 0.05|v|_{max}$ where v is the speed.

ing deposit. The three phases of the flow are illustrated in Figure 3, where the free-fall regime I is characterised by growing vertical kinetic energy, the heap-flow regime II by the conversion of vertical to radial kinetic energy and the shallow layer regime III by the gradual decline of the dominant radial kinetic energy.

The viscoplastic hypothesis (1) is made under the assumption that the volume fraction is constant in the limit of dense flows. As stress and strain rate tensors are extracted directly from the collapsing compressible flow data [21], we actually worked with the equivalent expression

$$\tau_{ij} = \eta \dot{\gamma}_{ij}^c \quad \text{where} \quad \dot{\gamma}_{ij}^c := \dot{\gamma}_{ij} - \frac{1}{3} \dot{\gamma}_{ii} \delta_{ij} \quad (2)$$

is simply the non-isotropic part of the rate-of-strain tensor. To test this modified hypothesis (2), $\boldsymbol{\tau}$ and $\dot{\boldsymbol{\gamma}}^c$ were calculated over the flow domain at 5 to 10 different times during a collapse and over collapses of various different aspect ratios. These were calculated using a standard coarse-graining approach (equation 5, [16]) using a step function weighting. Averages were calculated over tori around the axis of symmetry with a $3d \times 3d$ square cross-section in the (r, z) plane. This was possible because the flow is axisymmetric to a large degree ($E_k^\theta \ll E_k^z, E_k^r$, see Figure 3) and meant that a significant number of particles contributed to the average at any one time. For a typical snapshot of the flow, data was calculated at ≈ 500 points in a (r, z) grid (see Figure 4) determined by ensuring a 50% overlap between neighbouring $3d \times 3d$ boxes.

To test how close $\boldsymbol{\tau}$ and $\dot{\boldsymbol{\gamma}}^c$ were to being simple mul-

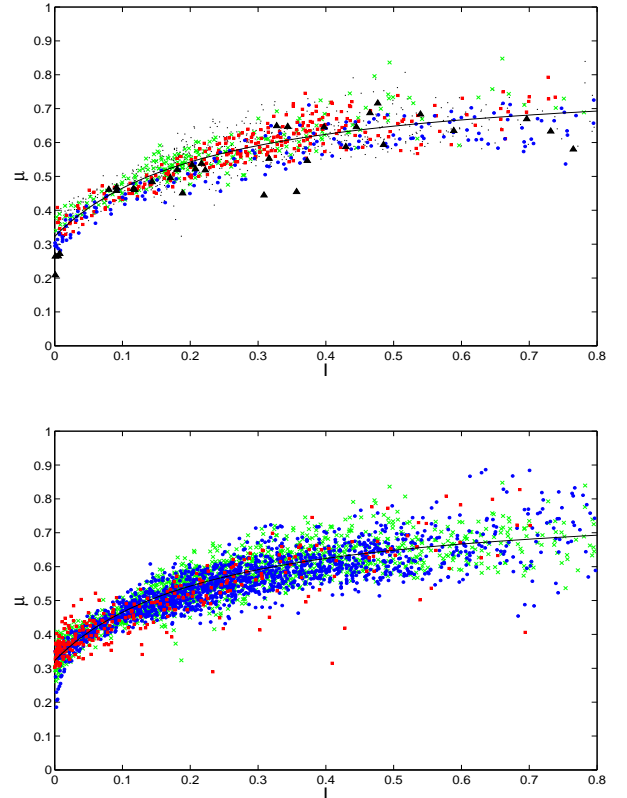


FIG. 5: μ against I for 3 different times at $a = 5$ (top: $t = 0.1s$ green crosses, $t = 0.18s$ red squares and $t = 0.26s$ blue dots with the remaining data at other times as small black dots; data with $\phi > 10^\circ$ indicated by black triangles) and 3 different geometries (bottom: $a = 1$ red squares, $a = 5$ green crosses and $a = 8$ blue dots). The curve is the best fit line of the form (3) with $\mu_m = 0.5$. The maximum shear estimator for η is used here but the plot is essentially the same using the second invariant instead.

tiples of each other, 2 estimators of η were used: $|\boldsymbol{\tau}|/|\dot{\boldsymbol{\gamma}}^c|$ where $|\boldsymbol{\tau}| = \sqrt{\frac{1}{2}\tau_{ij}\tau_{ij}}$ is the second invariant (similarly for $\dot{\boldsymbol{\gamma}}^c$), and the ratio of the maximum shear component $\tau_{\hat{r}\hat{z}}$ to $\dot{\gamma}_{\hat{r}\hat{z}}^c$ where \hat{r} and \hat{z} are the appropriately transformed coordinates (finding the orientation of the maximum shear was a good but not infallible way to predict the local flow direction). Only data for which the pressure exceeded 5% of the maximum were used to exclude the initial free-fall regime high in the column where the grains are not in frictional contact with each other (see Figure 4). Of the data points which remained, the principal axes of $\boldsymbol{\tau}$ and $\dot{\boldsymbol{\gamma}}^c$ were surprisingly well-aligned; 95% to within 10° . The misalignment that does occur is invariably at the low-density free surface and near low-speed regions (the axis of symmetry and the static-to-flowing interface): see Figure 4. No misalignment was found near the boundary except at the rapidly moving head which is also close to the free surface.

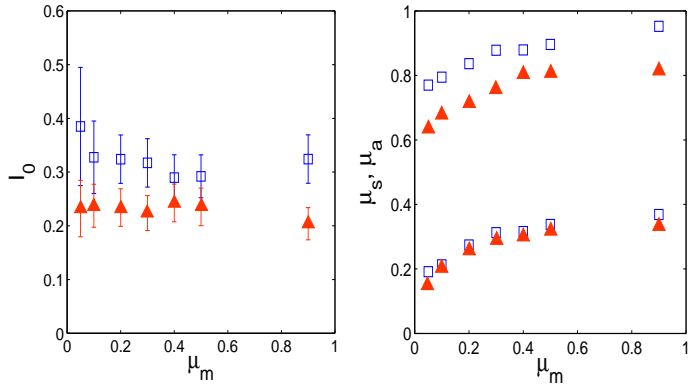


FIG. 6: The fitting parameters I_0 (left), μ_a (right, upper) and μ_s (right, lower) as a function of μ_m . Open squares from $|\tau|/|\dot{\gamma}^c|$ data and filled triangles from maximum shear data. Error bars are 95% confidence intervals (shown on the left, indicated by the size of symbol on the right).

Figure 5 shows how $\mu = \eta|\dot{\gamma}^c|/P$ varied with I for 3 different geometries and for 3 different times for the same geometry. The collapse onto a best fit line

$$\mu(I) = \mu_s + \frac{\mu_a - \mu_s}{I_0/I + 1} \quad (3)$$

as suggested by unidirectional flow experiments [2, 5, 17] is remarkable. There is clear evidence that not only is $\mu = \mu(I)$ but that the behaviour for steady unidirectional flows carries over to unsteady, multi-directional flows. The theory is expected to fail in the jamming limit ($I \rightarrow 0$) but no indication of this breakdown is seen in the data. The functional dependence of the *macroscopic* friction μ , parametrised by (I_0, μ_s, μ_a) , on the *microscopic* friction μ_m (see Figure 6) is smooth and robust to whether $|\tau|/|\dot{\gamma}^c|$ or the maximum shear rate data is used. The values which emerge for the parameters are also reassuringly close to those found in experiments ([18]; $\mu_s \approx 0.4$, $\mu_a \approx 0.7$ and $I_0 \approx 0.3$) and fairly robust against changing the bottom roughness (the diameter of the glued-on particles was varied from a ratio of 0.5 to 4 times that of the flowing spheres).

The general applicability of viscoplastic theory found here is, frankly, a surprise given a) the presence of a large growing static-flowing interface, b) the proximity of most of the fast flow to the rough bottom boundary and c) the existence of a large free surface. Certainly the misalignment between the principal axes of the local stress and strain rate tensors is most likely to be significant in these regions but still is never large ($< 20^\circ$ in the flowing regions). The major obstacle to a simple local rheology is, of course, non-local effects typified by the long range influence of boundaries. While this can be crucial for understanding steady flows [17], the extra presence of inertia in the momentum balance for transient flows appears to considerably reduce this influence.

The clear conclusion from this study is the ubiquity of the simple stress-strain rate relationship advocated by a simple viscoplastic continuum theory even in transient, multidirectional flow. Moreover, this relationship appears well fit with the experimental result for steady unidirectional flows and holds even near rough boundaries. This suggests that a simple viscoplastic modelling approach can be used to quantitatively capture granular flow properties (at least within $\pm 10\%$) in real geophysical and industrial applications.

The authors are grateful for helpful conversations with O. Pouliquen and J. Snoeijer, and thank E. Lajeunesse and H. Huppert for sharing their data. LL was supported by a Marie-Curie IntraEuropean fellowship.

* Laurent.Lacaze@imft.fr

† R.R.Kerswell@bristol.ac.uk

- [1] H. M. Jaeger, S. R. Nagel, and R. P. Behringer, *Rev. Mod. Phys.* **68**, 1259 (1996).
- [2] P. Jop, Y. Forterre, and O. Pouliquen, *Nature* **441**, 727 (2006).
- [3] F. da Cruz, S. Emam, M. Prochnow, J.-N. Roux, and F. Chevoir, *Phys. Rev. E* **72**, 021309 (2005).
- [4] G. Lois, A. Lemaitre, and J. Carlson, *Phys. Rev. E* **72**, 051303 (2005).
- [5] G. MiDi, *Eur. Phys. J. E* **14**, 341 (2004).
- [6] E. Lajeunesse, A. Mangeney-Castelnau, and J. P. Vilotte, *Phys. Fluids* **16**, 2371 (2004).
- [7] G. Lube, H. E. Huppert, R. S. J. Sparks, and M. A. Hallworth, *J. Fluid. Mech.* **508**, 175 (2004).
- [8] N. J. Balmforth and R. R. Kerswell, *J. Fluid Mech.* **538**, 399 (2005).
- [9] A. Mangeney-Castelnau, F. Bouchet, J. P. Vilotte, and E. Lajeunesse, *J. Geophys. Res.* **110**, B09103 (2005).
- [10] R. R. Kerswell, *Phys. Fluids* **17**, 057101 (2005).
- [11] E. Larrieu, L. Staron, and E. J. Hinch, *J. Fluid Mech.* **554**, 259 (2006).
- [12] L. Staron and E. J. Hinch, *J. Fluid Mech.* **545**, 1 (2005).
- [13] L. Staron and E. J. Hinch, *Granular Matter* **9**, 205 (2007).
- [14] R. Zenit, *Phys. Fluids* **17**, 031703 (2005).
- [15] L. Lacaze, J. C. Phillips, and R. R. Kerswell, *Phys. Fluids* **20**, 063302 (2008).
- [16] I. Goldhirsch and C. Goldenberg, *Eur. Phys. J. E* **9**, 245 (2002).
- [17] P. Jop, Y. Forterre, and O. Pouliquen, *J. Fluid. Mech.* **541**, 167 (2005).
- [18] Y. Forterre and O. Pouliquen, *Ann. Rev. Fluid Mech.* **40**, 1 (2008).
- [19] I is a variant (square root) of a previously-introduced Savage number (S.B.Savage & K.Hutter, *J. Fluid Mech.* **199**, 177, 1989) and the Coulomb number (C.Ancey, P.Coussot & P.Evesque, *J.Rheol.* **43**, 1673, 1999).
- [20] The commercially-available software EDEM was used: <http://www.dem-solutions.com>
- [21] The volume fraction is typically in the interval [0.46,0.62] but can decrease to 0.21 near a rapidly moving surface